Development of Caryopsis and Starch Physicochemical Properties in Different Grain Positions of Wheat Spikelets

Leilei Wang
Yangzhou University
Xurun Yu
Yangzhou University
Yong Zhang
Yangzhou University
Yunfei Wu
Yangzhou University
Fei Xiong (feixiong@yzu.edu.cn)
Yangzhou University

Research Article

Keywords: grain position, starch, protein, wheat

Posted Date: August 17th, 2021

DOI: https://doi.org/10.21203/rs.3.rs-763584/v1

Abstract

Background: Spikelets at different spike positions and the caryopsis at different grain positions grow and develop differently. The caryopsis development and physicochemical properties of starch at different grain positions (the first, second, and third grain positions: G1, G2, and G3) of wheat spikelets were investigated in this study.

Results: During the development process, the thickness of both dorsal and abdomen pericarp 8 days after anthesis (DAA) followed the sequence G2 < G1 < G3. However, at 14 DAA the thickness followed the dorsal sequence of G1 < G2 < G3 and the abdomen sequence of G2 < G1 < G3. At 20 and 30 DAA, no difference existed in the pericarp thickness of each grain. The accumulation quantities before 20 DAA varied with starch and protein of endosperm cell in the order G1 > G2 > G3. In mature caryopsis, the caryopsis size and weight indicate that G1 = G2 > G3. The starch content followed the order G1 > G2 > G3, while the essential amino acid, the total amino acid, and the protein content followed the order G2 > G1 > G3. The apparent amylose content followed the sequence G3 > G2 > G1, and A-type starch content followed G3 > G1 > G2. The amorphous ratio followed the order G2 > G1 > G3, whereas the double-helix ratio and the relative crystallinity exhibited the opposite trend. The order of the final degree of hydrolysis through AAG, PPA, and HCL was G2 > G1 > G3.

Conclusions: The different material contents were possibly due to the short development time of caryopsis, and the difference in starch physicochemical properties between G2 and the other grain positions might be related to the components and structural characteristics of starch.

1 Background

The final wheat grain yield can be described by studying and understanding the individual constituent parts (e.g., spikes/m^2, grain number/spike, and grain weight) [1]. The number and arrangement of spike components (e.g., spikelets) affect the spike length, the spike weight, the grain number and weight per spike, and the spikelet number per spike, which all contribute to the final grain yield per spike [2–4]. Significant asynchronous development exists in the different spike and grain positions of wheat. According to the grain positions and flowering time, inferior grains have poor quality and low grain weight, which severely restrict the quality and yield potential of wheat [5, 6]. Thus, the research on the developmental mechanism and control measures of inferior grains has received significant attention.

Wheat grain is a caryopsis where the ovary wall is fused to a single seed. In addition to the embryo, the endosperm, the seed coats, and the pericarp can be distinguished from the center to the periphery of the grain [7–9]. The pericarp, which lies on the outermost layers of the caryopsis, is composed of three layers, namely, the epicarp, the mesocarp, and the endocarp [10]. Xiong et al. studied the structural and physiological features of wheat pericarp development and found that pericarp starch granules accumulate in mesocarp cells 3 days after anthesis (DAA), reach maximum accumulation 9 DAA, and completely disappear after 15 DAA [11]. Studies have also reported that starch granules are synthesized in amyloplasts or chloroplasts from anthesis to 11 DAA but gradually disappear after 11 DAA [12]. Similar results have been reported by Yu et al. who pointed out that pericarp starch granules exhibit a typical accumulation peak 5 DAA and then gradually decompose until 22 DAA [13]. As the most important part of the grain, endosperm mainly accumulates substances, such as starch and protein. Starch accounts for 65–75% of the final dry weight of grains and serves as a multifunctional ingredient for the food industry [14]. A-type granules (> 9.9 μm) start to form in the amyloplast 4–5 DAA and continue to form until the end of the endosperm cell division phase [15]. The diameter of these early synthesized granules stops increasing 19 DAA, but the volume continues to increase [16]. B-type starch granules (< 9.9 μm) initiate 10–16 DAA [17, 18] and continue to enlarge until 21 DAA [19]. Starch granules with different sizes show different physical, chemical, and functional properties during endosperm development [20, 21]. The protein synthesis and accumulation in the endosperm mainly exist in the form of protein bodies (PBs). The PBs in wheat endosperm cells appear approximately 12 DAA and begin to synthesize in large quantities 16 DAA; the number increases rapidly, and the volume rises. In the late stage of maturity, the PBs are squeezed into a sheet structure due to the enrichment of amyloplasts in the endosperm cells and fill the gaps of the amyloplasts [22]. However, Yang et al. observed that proteins mainly form PBs via the Golgi apparatus in the vacuole at the early stage of wheat endosperm development and found that most proteins are derived from the rough endoplasmic reticulum 7 DAA [23]. Furthermore, they also found that the morphology of the PBs in sub-aleurone cells are

more and larger than the central endosperm [22, 23]. The above research is mainly focused on the accumulation of substances during the development of wheat caryopsis, while the research on the developmental differences of caryopsis at different grain positions is limited.

In recent years, domestic and foreign scholars have conducted research on different grain positions. Within the central spikelets, the weight at G2 is higher than that at G1, G3, and G4 when moving from the most proximal position to the most distal spikelet position [24, 25]. Dai found that the volume and surface area percentage of C-type granules and the protein content in basal grains are higher than those in distal grains, but those of the A, B-type granules in basal grains are lower than those in distal grains [26]. BOZ et al. found significant differences between the grain positions within the spike based on hectoliter weights [27]. Yu et al. indicated that grains at upper and basal spikelets can increase their weight by increasing the volume of B-type granules [28]. Within a spike, spikelets are unevenly distributed and largely different due to their unbalanced development [29]. Li et al. found that the effects of spikelet and grain positions on grain weight vary with the grain number of spikelets [30]. Li et al. analyzed the dynamic changes of the weight, protein accumulation, and protein content of superior and inferior grains [31]. The difference between superior and inferior grains filling is due to the ratio of carbon to nitrogen [32, 33], sink capacity [34], unbalanced endogenous hormone levels [35, 36], as well as the enzyme activities and genes expression involved in the conversion of sucrose to starch [37–39], and inconsistencies in assimilation transportation [40]. These studies focus on the protein content, the difference in starch granule size distribution, and the yield of different spike and grain positions, while comparative studies on the physicochemical properties of starch in different grain positions are limited.

Therefore, this study analyzed the accumulation of starch and protein during caryopsis development through microscopic observation techniques, such as slices, and the compositional differences and physicochemical properties of the two in the mature stage to provide a reference for the study of the grouting mechanism of different grain positions in wheat spikes and the regulation mechanism of individual grains.

2 Materials And Methods

2.1 Experimental Materials

The wheat variety “Yannong 19 (YN19)”, purchased from Lixiahe Agricultural Science Institute, Jiangsu Province, was planted in the experimental field in Yangzhou University from October 2017 to June 2018. The flowering wheat spikelets were marked with a black oily marker, and seeds were collected from different locations 8, 14, 20, and 30 DAA, and six grains were fixed in 2.5% glutaraldehyde solution for semi-thin sectioning. Starch was extracted from the grain 55 DAA to determine the physicochemical properties.

2.2 Production of semi-thin resin slices

The preparation of resin semi-thin sections refered to the method of Xiong et al. [11]. The steps were as follows: The fresh caryopsis was cut to a slice of 1-2 mm with a double-sided blade along the middle part, and then soaked in 2.5% glutaraldehyde solution for 48 h. The phosphate buffer (pH7.2) were used to clear the glutaraldehyde solution and did the dehydration step from 20% to 100% absolute ethanol series concentration. After the previous step, we replaced ethanol with propylene oxide, and finally gradually increased the concentration of the low-viscosity embedding medium (Spurr 1969) in a propylene oxide environment, and polymerize it into an embedded block in a pure resin at 70°C. We used a semi-thin microtome (Leica Ultracut R, Germany) to make 1 μm thick sections, evaporated water of the sections stained with 0.5% methyl violet for 30 seconds on a dryer, and observed and photographed under Leica DMLS microscopy.

2.3 Determination of protein and amino acid content

The protein content is analyzed using the CHN mode of the elemental analyzer (Vario EL cube, German element manufacturer, Germany) to analyze the total nitrogen content, and the result is multiplied by the coefficient 6.25 to obtain the protein content.

The amino acid content was determined using the principle of ninhydrin reaction (the ninhydrin reagent kit was purchased from Biochrome Company, UK) and measured by the amino acid analyzer of the Agricultural College of Yangzhou University.

2.4 Extraction of starch and total starch and amylose content determination

The separation of starch by water extraction method and total starch content was based on the test method of Wang et al. [5]. The apparent amylose content was determined by He et al. [41].

2.5 Morphology observation and granule size distribution analysis

The sample processing of starch morphology observation refers to the research method of Yu et al. [13]. We sucked 10 μL of anhydrous ethanol-dispersed starch mixture into a fluted sample stage wrapped in tin foil. After ethanol evaporated in the room temperature, gold plating was performed in the etching coater (BAL-TEC SCD 500 Sputter Coater, Leica, Germany). The sample stage was placed under a scanning electron microscope (S4800, Hitachi, Japan) to observe the morphology of starch granules. The granule size distribution of the starch were determined using a MS-2000 laser diffraction particle size analyzer (Malvern Corporation, England). Approximately 50 mg of starch was weighed into 10-ml (Eppendorf) tubes and suspended with 5 ml of double-distilled water. The equivalent volume, the equivalent surface area, and the proportions of starch granules were automatically assessed using a laser diffraction particle size analyzer (Mastersizer 2000), and the diameter of a sphere with the same volume as the starch grain and the diameter of a circle with the same projected area as the real starch grain were measured.

2.6 XRD analysis

We use a glass slide to compact a little dried starch sample on the stage, and place the stage on the X-ray diffractometer (D8 Advance, Bruker, Germany) to scan the spectrum, where the scanning range was 3° - 40° and the scanning step length was 0.4 s. The calculation method of relative crystallinity was based on Nara and Komiya [42]. The difference was just that the software version was Photoshop CS6 and Image-Pro-Plus image analysis software.

2.7 ^{13}C CP/MAS NMR analysis

The ^{13}C Cross Polarization/Magic Angle Spinning Nuclear magnetic resonance (^{13}C CP/MAS NMR) spectrometer (ADVANCE

2.8 Fourier transform far infrared spectroscopy

The pretreatment of the sample was 30 mg starch mixed with 100 microliters of distilled water to form a paste. The scanning of spectrum background was done with distilled water first, and then added the paste with a small spoon to the sample stage of the Fourier Transform Far-Infrared Spectrometer (FTIR; 7000, Varian, USA) to scan the sample spectrum, and the range was 800-4000 cm^{-1}. In the next step, the spectrum processing referred to the method of Wei et al. [17]. The image production was performed with Origin8.0 and the ratio of (1045/1022) and (1022/995) cm^{-1} was calculated based on the peak intensity at 1045, 1022, 995 cm^{-1} and repeated three times.

2.9 Starch hydrolysis determination

Starch hydrolysis was determined using the method of Wang et al. [45]. After centrifugation (3000 × *g*) at 4 °C for 10 min, the soluble sugar content [M (mg)] obtained by hydrolysis in the supernatant is determined by the sulfuric acid-anthrone colorimetric method of Wei et al. [17]:

Amount of hydrolyzed starch = M × 0.9.

2.10 Statistical analysis

The standard error of data was analyzed using the SPSS 19.0 software, and the differences in measured values among the different starch samples were tested at $P < 0.05$.

3 Results

3.1 Observation of the microstructure of pericarp at different developmental stages

According to the structural characteristics of wheat caryopsis, we observed two parts, namely, the abdomen region with a symmetrical structure and the opposite dorsal region (Fig. 1). The pericarp structure indicates that the thicknesses of the abdomen and dorsal pericarps at different grain positions vary. Eight DAA (Figs. 1A–C, a–c), the thickness of the pericarp on the abdomen and dorsal followed the order G3 > G1 > G2. The large thickness cleared the late start of development. The change in pericarp thickness and the large cavities in the mesocarp were mainly due to the programmed cell death during the development of the pricarp cells. Fourteen DAA (Figs. 1D–F, d–f), the thickness of the abdomen pericarp still followed G3 > G1 > G2, while that of the dorsal pericarp changed to G3 > G2 > G1, revealing that the dorsal pericarp of G1 developed faster than those of the other grains. Twenty DAA (Figs. 1G–I, g–i), the dorsal pericarp thickness of the three grain positions was significantly thicker than that of the abdomen, but no difference in the pericarp thickness in the same region was observed. Thirty DAA (Figs. 1J–L, j–l), no significant difference in pericarp thickness between the two regions of the three grain positions was observed. The above results show an obvious sequence of starting points for the pericarp development of different grain positions, and the development duration varied, which is closely related to the filling process of the caryopsis at each grain position.

3.2 Microstructure observation of endosperm cells in different developmental stages

Eight DAA (Figs. 2 A, E, I), the endosperm cells of the three grains all appeared as spindle-shaped starch granules, which were squeezed by vacuoles at the edge of the cells. However, the quantity and size of the starch granules were obviously different. G1 displayed the most and the biggest starch granules and a certain swelling, followed by G2 and G3. Furthermore, no PB deposition was observed in G2 and G3. Fourteen DAA (Figs. 2 B, F, J), more large starch grains and small spherical starch grains have accumulated in the three grain positions. However, the number of small starch grains in G1 was the highest and that in G3 was the lowest. Generally, small starch grains are formed by the splitting of large starch grains [16]. In terms of protein, G1 had the largest number of and enlarged PBs, whereas G2 and G3 mostly had small PBs. Twenty DAA (Figs. 2 C, G, K), the number of large starch granules did not change significantly, while the number of small starch granules increased further, and the number of granules in G1 and G3 was significantly greater than that of G2. Thirty DAA (Figs. 2 D, H, L), G1 was nearly filled with amyloplast and PBs, which were also squeezed to fill the gaps between starches. Meanwhile, regular spherical PBs could still be observed at G2, and many gaps existed between the amyloplast and PBs at G3, indicating that the fullness of G3 was significantly less than that of G1 and G2. The above results demonstrate that the development of endosperm cells follows an obvious sequence of grain positions, which ultimately determines the length of development time.

3.3 Analysis of material content and characteristics in mature stage

3.4 Observation of Grain Morphology and Measurement of Agronomic Characters

In this study, the large spike wheat YN19 was selected to separate the three grains in the spikelet as the fourth and fifth grain positions without grains (Figs. 3A–C), and the grain size was measured and analyzed (Figs. 3D–E). The picture (Figs. 3D–E) shows that the grain length and width of G3 were obviously smaller than those of the other two positions, while the length of G1 was slightly larger than that of G2, and the width of G2 was slightly larger than that of G1. Through precise measurement (Tab. 1), no significant difference was observed in the grain size and weight of G1 and G2, while those of G3 are significantly smaller than those of G1 and G2.

Table1

Size parameters of mature grains at different grain positions

Sample	Length (cm)	Wide (cm)	Thick (cm)	1000-grain weight(g)
G1	7.55±0.15 a	3.50±0.04 a	3.28±0.09 a	55.65±1.75 a
G2	7.60±0.13 a	3.57±0.06 a	3.25±0.17 a	55.95±0.95 a
G3	7.06±0.14 b	3.20±0.05 b	2.78±0.05 b	42.68±1.98 b

The values in the table are the average of the three replicate values, and the same column data with different letters indicates significant difference between the two ($p < 0.05$).

3.5 Determination of Amino Acid Content in Grains

In nutrition, amino acids are classified as either essential or non-essential amino acids [46]. Essential amino acids, also known as indispensable amino acids, are a group of amino acids that humans and other vertebrates cannot synthesize from metabolic intermediates. We found evident differences in amino acids content, which are mainly manifested as the highest Aspartice acid, Serine, Glutamic acid, Cryteine, Valine, Methionine, Isoleucine, Leucine, and Histidine content at G2, which ultimately leads to G2 having the highest content of essential and non-essential amino acids (Fig. 4A). The essential amino acids and total amino acid in G1 were lower than those in G3 (Fig. 4B). The result is the parameter difference under unit mass, which is converted to the protein content within a single grain followed the sequence G2 > G1 > G3 (Fig. 4C).

3.6 Determination of starch particle size distribution in different grain positions

The granule size distribution in wheat starch is an important factor affecting the end-use quality. According to the granule size, the endosperm starch was divided into B-type granules (diameter < 9.9 μm) and A-type granules (diameter > 9.9 μm) [47]. As shown in Figure 5A, the volume-type diameter parameters of the different grain positions of wheat show a weak difference between G1 and G2, but G3 exhibited a significant difference between the two ranges, namely, 2.8–9.9 μm and 22.8–42.8 μm. The results indicate that the number of small starch granules in G3 was less than those in G1 and G2, but the number of large starch granules was greater than those of the two. Similar results can be seen from the results of the scanning electron microscopy of starch (Figs. 5B, C, D). Interestingly, the data indicates that A-type, Area average granule size and the Volume average granule size were significantly different among the three positions and followed the sequence G3 > G1 > G2, whereas the B-type starch granule size followed the order G2 > G1 > G3 (Tab. 2).

Table 2

Particle size analysis of starch granules

Sample	B-type (< 9.9 μm)	A-type (> 9.9 μm)	Area average granule size D[3,2]	Volume average granule size D[4,3]
G1	36.02b	63.98b	7.043b	17.799b
G2	38.22a	61.78c	6.995c	17.263c
G3	28.60c	71.40a	7.572a	18.997a

The values in the table are the average of three replicate values, and the same column data with different letters indicates a significant difference between the two ($p < 0.05$).

3.7 Analysis of the structure of starch in different grain positions

According to previous studies, the structural characteristics of starch are mainly reflected in three aspects: the content of components, the order of surface structure, and the degree of crystallinity. The components are mainly amylose and amylopectin. In this study, the apparent amylose content of G1 was the lowest, followed by G2, and that of G3 was the highest (Tab. 3). ^{13}C CP/MAS NMR spectroscopy is widely used for studying the structure of starch samples, kinetics, and correlation. The single- and double-helix contents formed a crystalline structure, and the amorphous region formed an amorphous structure. Figure 6A indicates that the ^{13}C CP/MAS NMR spectrum of starch has four main resonance peaks (i.e., 103, 82, 73, and 62 ppm) in the range of 50–120 ppm. Software analysis shows that the amorphous starch proportion of G2 was the highest, followed by G1 and G3; the single-helical starch ratio of G3 was the highest, followed by G2 and G1, and the double helix ratio followed the order G3 > G1 > G2 (Tab. 3). The results of Fourier transform infrared spectroscopy show that G1 > G2 = G3 in the ratio of 1045/1022 and G1 < G2 = G3 of the 1022/995 ratio (Fig. 6C, Tab. 3). The crystallinity of starch was analyzed through the X-ray diffraction spectrum. Obvious characteristic peaks were observed at 15°, 17°, 18°, and 23° of the spectrum, which are typically A-type crystal peaks (Fig. 6D). Data processing results show that G3 exhibited the highest relative crystallinity, followed by G1, and that of G2 was the lowest (Tab. 3). The above results indicate significant differences in the order degree of the surface and crystal structures of starch at different grain positions.

Table 3

Relative proportions of starch single helix, double helix and amorphous structure

Sample	Amorphous ratio	Single-helical ratio	Double-helix ratio	1045/1022 (cm^{-1})	1022/995 (cm^{-1})	RC (%)	AAC (%)
G1	48.58±0.74b	5.18±0.08a	46.24±0.71b	0.702±0.042a	1.132±0.038b	14.98±0.10b	20.75±1.16c
G2	50.21±0.66a	5.03±0.22a	44.76±0.65c	0.612±0.031b	1.201±0.033a	12.68±0.21c	23.53±0.48b
G3	45.77±0.81c	4.15±0.21b	50.08±0.68a	0.558±0.025b	1.252±0.045a	15.45±0.13a	25.24±1.02a

The values in the table are the average of three replicate values, and the same column data with different letters indicates significant difference between the two ($p<0.05$).

3.8 Hydrolysis of starch

The hydrolysis process of starch is divided into two stages: the early rapid and late slow hydrolysis stages. The results of the study indicate that the three hydrolysis modes exhibited two stages, namely, the rapid and slow hydrolysis stages (Fig. 7). In the rapid hydrolysis stage, the hydrolysis times of the three granular starches were 0–4, 0–6, and 0–6 days (Fig. 7A), the hydrolysis times using porcine pancreatic alpha-amylase (PPA) were 0–12, 0–24, and 0–8 h (Fig. 7B), and the hydrolysis times through

Aspergillus niger amyloglucosidase (AAG) were 0–8, 0–6, and 0–8 h (Fig. 7C). In the same hydrolysis mode, the order of final hydrolysis of starch was G2 > G1 > G3 (Fig. 7).

4. Discussion

Significant sequence of caryopsis development existed in different grain positions

Wheat caryopsis can distinguish the endosperm, the seed coats, and the pericarp [7; 8; 9]. Pericarp is composed of three parts: epicarp, mesocarp, and endocarp [10]. This study mainly observed the pericarp thickness of different grain positions at different developmental stages. The change in pericarp thickness in the development of caryopsis was due to two factors: the degradation of the mesocarp caused by the programmed cell death of pericarps, and the enrichment and extrusion of endosperm cells [12]. Eight DAA (Fig. 1), the thickness of G2 was significantly smaller than those of the other grain positions, while the thickness of G3 was significantly larger than the other grain positions. Until 20 DAA (Fig. 1), the thickness of each grain position showed no obvious difference. Thirty DAA (Fig. 1), the mesocarp basically disappeared, while the cell walls of the exocarp and the endocarp thickened. Pericarp cells eventually become dead cells that coat the surface of the grain [12]. These change disciplines of pericarp thickness verify that the development cycle of pericarp followed the order G2 > G1 > G3. The delay of PCD in pericarp cells may be due to the sufficient photosynthetic assimilates and energy supply [12]. The physiological and anatomical functions of the pericarp are similar to those of leaves and resemble those of storage organs [48]. Similar reports pointed out that wheat pericarp has many functions, such as protection, photosynthesis, mineral accumulation, synthesis, and degradation of starch during the development process [11, 12]. The development of pericarp is closely related to the process of transport and accumulation of caryopsis, and these differences in pericarp development largely affect the accumulation of starch and protein.

Endosperm is the most important place for the accumulation of storage materials. The endosperm is full of starch in the form of amyloplast and protein in the form of PB, both of which account for more than 80% of the total dry weight [14]. The accumulation of starch grains starts at 4–5 DAA [15]. In this study, 8 DAA (Fig. 2), all three grain positions accumulated amyloplast with differences in number and size, indicating that the developmental starting points of different grain positions varied. Both were also closely related to the flowering time of each grain position. The accumulation of protein was relatively late. A study observed that PB was 7 DAA [23], and another one study found PB was 12 DAA [22]. Protein accumulation was observed in G1 and G2 but not in G3. Fourteen DAA (Fig. 2), the starch granule in each grain position increased in size into A-type starch granules. Studies show that A-type starch granules will continue to increase until 19 DAA [16]. Many small starch granules, that is, B-type starch granules were also observed, which is basically consistent with the previous belief that B-type starch granules originated from 10–16 DAA [17, 18]. At 20 DAA (Fig. 2), the amyloplast and PBs in the endosperm were further enlarged and increased. The number of small starch granules in G2 was significantly less than those in the other grain positions, while the number of PBs was more than those in the other grain positions, indicating that the B-type starch grains at G2 were enriched later than the other grains. Thirty DAA (Fig. 2), G1 and G2 were basically enriched, while many gaps in G3 were unfilled. The protein at G1 was squeezed in the gaps between starches, which is consistent with the observation of Zhou et al. during the maturation period [22]. The above results indicate that the delayed formation of B-type starch grains and the increased accumulation of PBs in the middle stage of development (approximately 20 DAA) of the grains at G2 and the poor filling degree of G3 ultimately lead to the starch content order G1 > G2 > G3 and the protein content order G2 > G1 > G3 in the mature grains. The difference in the development and content of starch and protein was largely due to the final grain length, width, thickness, and grain weight expressed as G1 = G2 > G3.

In nutrition, amino acids classify as either essential or non-essential amino acids. These classifications were a result of early studies on human nutrition [46]. Essential amino acids refer to amino acids that the human body cannot synthesize by itself or whose synthesis speed cannot meet the needs of the human body and must be ingested from food [49]. In this study, the content of most of the amino acids at G2 was greater than those of the other grain positions. Meanwhile, the difference between G1 and G3 was mainly manifested in the content of essential amino acids, and the content of G3 was higher than that of

G1. However, the protein content in a single grain followed the order G2 > G1 > G3 because the grain weight of G3 was significantly smaller than those of the other positions (Fig. 3). The above comparison of nutrient content can also provide reference for eating and processing wheat.

The structure and physicochemical properties of starch in G2 were quite different from those in the other grain positions

Starch is the substance with the largest proportion of caryopsis dry weight, whose characteristics will directly affect quality and use. Starch is composed of two major glucose polymers, namely, amylose and amylopectin [50]. This study found that the amylose content increased with the grain size. The seed endosperms exhibited a unique bimodal starch granule size distribution: B-type granules (diameter < 9.9 μm) and A-type granules (diameter > 9.9 μm) in mature wheat grains [51, 52]. Given the separation and quantification limitations, C-type starch granules (diameter < 5 μm) are usually classified as B-type starch granules [53–55]. The analysis of starch granule size indicates that the proportion of A-type starch in each grain position, the area average particle size [3, 2], and the volume average particle size [4, 3] all followed the position sequence G3 > G1 > G2, while the ratio of B-type starch granules exhibited an opposite trend. The research of Yu et al. revealed a similar result, that is, the ratio of amylase to amylopectin is positively correlated with the volume proportion of 22.8–42.8 μm but negatively related to the volume proportion of < 9.9 μm [28]. With the development of modern technology, CP/MAS ^{13}C NMR spectroscopy, XRD, and ATR-FTIR have been successfully used to study the long-range ordered structures of whole granules and the short-range ordered structures of the external regions of starch granules [56, 57]. The ATR-FTIR absorption bands at 1045 and 1022 cm^{-1} are associated with crystalline lamellar and amorphous structures, respectively, while the band at 995 cm^{-1} is attributed to the bending vibrations of C–OH bonds [58]. The IR ratios of 1045 cm^{-1}/1022 cm^{-1} and 1022 cm^{-1}/995 cm^{-1} are considered quantitative indices for evaluating the short-range ordered structures of starch granules [59]. The results show that the relative crystallinity and the double helix ratio follow the sequence G3 > G1 > G2, while the amorphous ratio shows the opposite trend. The 1045 cm^{-1}/1022 cm^{-1} of G1 showed a larger position than the other grain positions, while 1022 cm^{-1}/995 cm^{-1} showed a smaller G1 position than the others. These results indicate that G3 had higher crystallinity and order of surface structure, while G2 had the lowest.

Starch hydrolysis is complex because it is closely related to the physical and chemical properties of starch grains [60]. The susceptibility of starch to acid and enzyme hydrolysis was influenced by factors, such as amylase content, crystalline structure, granule size, and relative surface area of granules [60, 61]. G2 had the largest ratio of B-type starch with a high surface area to volume ratio [62], which exhibited a large contact area with enzymes and acids and accelerated starch hydrolysis. The highest amorphous starch ratio and lowest relative crystallinity of G2 made it less resistant to enzymatic and acid hydrolysis, resulting in the following degree of hydrolysis: G2 > G1 > G3.

5. Conclusion

The differences of the grain positions in wheat spikelets were mainly manifested in two aspects: structure and properties. The pericarp development on the dorsal and abdomen at G2 was early and long, and G3 developed later within a short duration. The order of endosperm cell enrichment and the total starch content in the mature stage followed G1 > G2 > G3, whereas the amino acid and protein contents were G2 > G3 > G1. Compared with other grain positions, G2 has a high B-type starch granule content and an amorphous structure, resulting in the highest degree of hydrolysis at G2 and the lowest at G3.

Abbreviations

^{13}C CP/MAS NMR: ^{13}C Cross Polarization/Magic Angle Spinning Nuclear magnetic resonance; AAC: apparent amylose content; AAG: *Aspergillus niger* amyloglucosidase; ATR-FTIR: attenuated total reflectance-Fourier transform infrared; DAA: days after anthesis; G1, G2, and G3: the first, second, and third grain positions; PBs: protein bodies; PPA: porcine pancreatic alpha-amylase; RVA: rapid viscosity XRD: X-ray diffraction; YN19: Yannong19.

Declarations

Ethics approval and consent to participate

Not applicable

Consent for publication

Not applicable

Availability of data and material

All data generated or analyzed during this study are included in this manuscript.

Competing intends

The authors declare that they have no competing interests.

Funding

This study was supported by the Natural Science Foundation of China (31971810, 31801269) and A Project Funded by the Priority Academic Program Development of Jiangsu Higher Education Institutions (PAPD).

Authors' contributions

LW : Participated in the main test process and the writing and checking of the paper; XY : Provided experimental materials, and put forward valuable suggestions for revision of the first draft of the paper, and provided partial funding for this paper; YZ : Participated Part of the test process and data processing; YW : Participated in the English proofreading and proposed some revision suggestions; FX : Provide ideas and main funding for this paper.

Acknowledgements

Not applicable

References

1. Jemima, B., & Cristobal, U. A reductionist approach to dissecting grain weight and yield in wheat. JOURNAL OF INTEGRATIVE PLANT BIOLOGY. 2019; (3): 337–358.
2. Millet E. Relationships between grain weight and the size of floret cavity in the wheat spike. Ann. Bot. 1986; 58: 417–423.
3. Fischer RA. Hille-RisLambers D. Efect of environment and cultivar on source limitation to grain weight in wheat. Aust. J. Agric. Res. 1978; 29: 443–458.
4. Guo Z, et al. Genome-wide association analyses of 54 traits identifed multiple loci for the determination of foret fertility in wheat. New Phytol. 2017; 214: 257–270.
5. Wang L, Lin G, Yu X, et al. Endosperm enrichment and physicochemical properties of superior and inferior grain starch in super hybrid rice. Plant Biology, 2020; 22: 669–678.
6. Zhu D, Fang C, Qian Z, et al. Differences in starch structure, physicochemical properties and texture characteristics in superior and inferior grains of rice varieties with different amylose contents. Food Hydrocolloids. 2020; 110: 106170.

7. Bradbury D, MacMasters MM, Cull IM. Structure of the mature wheat kernel II Microscopic structure of pericarp, seed coat, and other coverings of endosperm and germ of hard red winter wheat. Cereal Chem.1956; 33: 342–360.
8. Bacic A, Harris PJ, Stone BA. Structure and function of plant cell wall. In The Biochemistry of Plant; Cambridge. 1988; pp: 297 – 371.
9. Zheng Y, Wang Z. The cereal starch endosperm development and its relationship with other endosperm tissues and embryo. Protoplasma. 2015; 252: 33–40.
10. Brillouet JM, Joseleau JP. Investigation of the structure of a heteroxylan from the outer pericarp (beeswing bran) of wheat kernel. Carbohydrate Research. 1987; 159: 109–126.
11. Xiong F, Yu X, Zhou L, Wang F, Xiong AS. Structural and physiological characterization during wheat pericarp development. Plant Cell Reports. 2013; 32: 1309–1320.
12. Zhou Z, Wang L, Li J, Song X, Yang C. Study on programmed cell death and dynamic changes of starch accumulation in pericarp cells of Triticum aestivum L. Protoplasma. 2009; 236: 49–58.
13. Yu X, Zhou L, Zhang J, Yu H, Xiong F, Wang Z. Comparison of starch granule development and physicochemical properties of starches in wheat pericarp and endosperm. Journal of the Science of Food and Agriculture. 2015; 95: 148–157.
14. Abdel-Aal ESM, Hucl P, Chibbar RN, Han HL, Demeke T. Physicochemical and structural characteristics of flours and starches from waxy and non-waxy wheats. Cereal Chem. 2002; 79: 458–464.
15. Dai Z. Activities of enzymes involved in starch synthesis in wheat grains differing in starch content. Russ J Plant Physiol. 2010; 57: 74–78.
16. Geetika A, Sarita J, Pierre H, Ravindra NC. Wheat genome specific granule-bound starch synthase I differentially influence grain starch synthesis. Carbohydr Polym. 2014; 114: 87–94.
17. Wei CX, Zhang J, Chen YF, Zhou WD, Xu B, Wang YP, Chen JM. Physicochemical properties and development of wheat large and small starch granules during endosperm development. Acta Physiol Plant. 2010; 32: 905–916.
18. Li WH, Shan YL, Xiao XL, Luo QG, Zheng JM, Ouyang SH, Zhang GQ. Physicochemical properties of A- and B-starch granules isolated from hard red and soft red winter wheat. J Agric Food Chem. 2013; 61: 6477–6484
19. Bechtel DB, Zayas I, Kaleikau L, Pomeranz Y. Size distribution of wheat starch granules during endosperm development. Cereal Chem. 1990; 67: 59–63.
20. Chiotelli E, Meste ML. Effect of small and the large wheat starch granules on thermo mechanical behavior of starch. Cereal Chem. 2002; 79: 286–293.
21. Park SH, Wilson JD, Chung OK, Seib PA. Size distribution and properties of wheat starch granules in relation to crumb grain score of pup-loaf bread. Cereal Chem. 2004; 81: 699–704.
22. Zhou R, Zhang Y, Li A, et al., Effect of booting nitrogen on accumulation of grain protein components and development of protein body in wheat. Journal of Triticeae Crops, 2009; 29(6): 1022–1026.
23. Yang Y, Chen X, Ran L, et al. Formation of protein bodies and the response to nitrogen in different positions during wheat endosperm development. J. Plant Biol. 2019; 62: 274–285.
24. Pan J, Jiang D, Cao WX, Sun CF. Effects of spikelet and grain positions on grain number, weight and protein content of wheat spike. Acta Agron Sin. 2005; 31: 431–437.
25. Pei XX, Wang JA, Dang JY, Wang XB, Zhang DY. Effects of spikelet and grain position on fertile spikelet number, grain weight and quality of wheat. Sci Agric Sin. 2008; 41: 381–390.
26. Dai Z. Starch granule size distribution in grains at different positions on the spike of wheat (*triticum aestivuml.*). Starch – Stärke. 2009; 61(10): 8.
27. BOZ H, Gercekaslan KE, KARAOĞLU MM, KOTANCILAR HG. Differences in some physical and chemical properties of wheat grains from different parts within the spike. Turkish Journal of Agriculture and Forestry. 2012; 36(3): 309–316.
28. Yu A, Li Y, Ni Y, Yang W, Yang D, Cui Z, et al. Differences of starch granule distribution in grains from different spikelet positions in winter wheat. Plos One, 2014; 9(12): e114342.

29. Ferrante A, Savin R, Slafer GA. Relationship between fruiting efficiency and grain weight in durum wheat. Field Crops Res. 2015; 177: 109–116.
30. Li Y, Cui Z, Ni Y, Zheng M, Yang D, Min J, et al. Plant density effect on grain number and weight of two winter wheat cultivars at different spikelet and grain positions. Plos One, 2016; 11(5): e0155351.
31. Li H, et al. Effects of spikelet and grain positions on grain weight and protein content of different wheat varieties. ACTA AGRONOMICA SINICA, 2017; 43(2): 238–252.
32. Murty P, Murty K. Spikelet sterility in relation to nitrogen and carbohydrate contents in rice. Indian J. Plant Physiol. 1982; 25: 40–48.
33. Wang Y. Effectiveness of supplied nitrogen at the primordial panicle stage on rice characteristics and yields. Int Rice Res Newsl. 1981; 6: 23–24.
34. Kato T. Effect of spikelet removal on the grain filling of Akenohoshi, a rice cultivar with numerous spikelets in a panicle. J Agric Sci. 2004; 142(2): 177–181.
35. Yang J, Zhang J. Grain filling of cereals under soil drying. New phytologist. 2006; 169(2): 223–236.
36. Zhang H, Tan G, Yang L, Yang J, Zhang J, Zhao B. Hormones in the grains and roots in relation to postanthesis development of inferior and superior spikelets in japonica/indica hybrid rice. Plant Physiol. Bio. 2009; 47(3): 195–204.
37. Jeng T, Wang C, Chen C, Sung J. Effects of grain position on the panicle on starch biosynthetic enzyme activity in developing grains of rice cultivar Tainung 67 and its NaN 3-induced mutant. J Agric Sci. 2003; 141(3–4): 303–311.
38. Ishimaru T, Hirose T, Matsuda T, Goto A, Takahashi K, Sasaki H, et al. Expression patterns of genes encoding carbohydrate-metabolizing enzymes and their relationship to grain filling in rice (Oryza sativa L.): comparison of caryopses located at different positions in a panicle. Plant Cell Physiol. 2005; 46(4): 620–628.
39. Wang E, Wang J, Zhu X, Hao W, Wang L, Li Q, et al. Control of rice grain-filling and yield by a gene with a potential signature of domestication. Nat Genet. 2008; 40(11): 1370–1374.
40. Serrago RA, Alzueta I, Savin R, Slafer GA. Understanding grain yield responses to source–sink ratios during grain filling in wheat and barley under contrasting environments. Field Crops Res. 2013; 150: 42–51.
41. He JF, Goyal R, Laroche A, et al. Water stress during grain development affects starch synthesis, composition and physicochemical properties in triticale. Journal of Cereal Science. 2012; 56(3): 552–560.
42. Nara S, Komiya T, Studies on the relationship between water-satured state and crystallinity by the diffraction method for moistened potato starch. Starch-Stärke. 1983; 35: 407–410.
43. Atichokudomchai N, Varavinit S, Chinachoti P. A study of ordered structure in acid-modified tapioca starch by ^{13} C CP/MAS solid-state NMR. Carbohyd. Polym. 2004; 58: 383–389.
44. Tan I, Flanagan BM, Halley PJ, Whittaker AK, Gidley MJ. A method for estimating the nature and relative proportions of amorphous, single, and double-helical components in starch granules by ^{13}C CP/MAS NMR. Biomacromolecules. 2007; 8: 885–891.
45. Wang L, Yu X, Yang Y, et al. Morphology and Physicochemical Properties of Starch in Wheat Superior and Inferior Grains. Starch-Stärke, 2017; 1700135.
46. Lopez MJ, Mohiuddin SS. Biochemistry, Essential Amino Acids. In StatPearls. StatPearls Publishing. 2021
47. Soulaka AB, Morrison WR. The amylose and lipid content, dimensions, and gelatinization characteristics of some wheat starches and their A- and B-granule fractions. J Sci Food Agr. 1985; 36: 709–718.
48. Müntz K, Rudolph A, Schlesier G, Silhengst P. The function of the pericarp in fruits of crop legumes. Die Kulturpflanz. 1978; 26: 37–67.
49. Peter, Fürst, Peter, Stehle. What are the essential elements needed for the determination of amino acid requirements in humans? Journal of Nutrition. 2004.
50. Slade AJ, McGuire C, Loeffler D, Mullenberg J, Skinner W, Fazio G, et al. Development of high amylose wheat through TILLING. BMC Plant Biology. 2012; 12:69.

51. Vermeylen R, Goderis B, Reynaers H, Delcour JA. Gelatinisation related structural aspects of small and large wheat starch granules. Carbohydr Polym. 2005; 62: 170–181.
52. Kim HS, Huber KC. Channels within soft wheat starch A- and B-type granules. J Cereal Sci. 2008; 48: 159–172.
53. Stamova BS, Laudencia-Chingcuanco D, Beckles DM. Transcriptomic analysis of starch biosynthesis in the developing grain of hexaploid wheat. Int J Plant Genomics.2012; 2009:407–426.
54. Asare EK, Jaiswal S, Maley J, Båga M, Sammynaiken R, Rossnagel BG, Chibbar RN. Barley grain constituents, starch composition, and structure afect starch in vitro enzymatic hydrolysis. J Agric Food Chem. 2011; 59: 4743–4754.
55. Ahmed Z, Tetlow IJ, Falk DE, Liu Q, Emes MJ. Resistant starch content is related to granule size in barley. Cereal Chem. 2016; 93: 618–630.
56. Yang Y, Tao W-Y. Effects of lactic acid fermentation on FT-IR and pasting properties of rice flour. Food Research Internationa. 2008; l41: 937–940.
57. Huang C, Lin M, Wang C. Changes in morphological, thermal and pasting properties of yam (Dioscorea alata) starch during growth. Carbohydrate Polymers. 2006; 64: 524–531.
58. Mutungi C, Onyango C, Doert T, Paasch S, Thiele S, Machill S, et al. Long- and short-range structural changes of recrystallised cassava starch subjected to in vitro digestion. Food Hydrocolloids. 2011; 25: 477–485.
59. Sevenou O, Hill SE, Farhat IA, Mitchell JR. Organisation of the external region of the starch granule as determined by infrared spectroscopy. International Journal of Biological Macromolecules. 2002; 31: 79–85.
60. Blazek J, Gilbert EP. Effect of enzymatic hydrolysis on native starch granule structure. Biomacromolecules 2010; 11: 3275–3289.
61. Huang J, Shang Z, Man J, Liu Q, et al. Comparison of molecular structures and functional properties of high-amylose starches from rice transgenic line and commercial maize. Food Hydrocolloid. 2015; 46: 172–179.
62. Bertoft E, Manelius R, A method for the study of the enzymatic hydrolysis of starch granules. Carbohyd. Res. 1992; 227: 269–283.

Figures

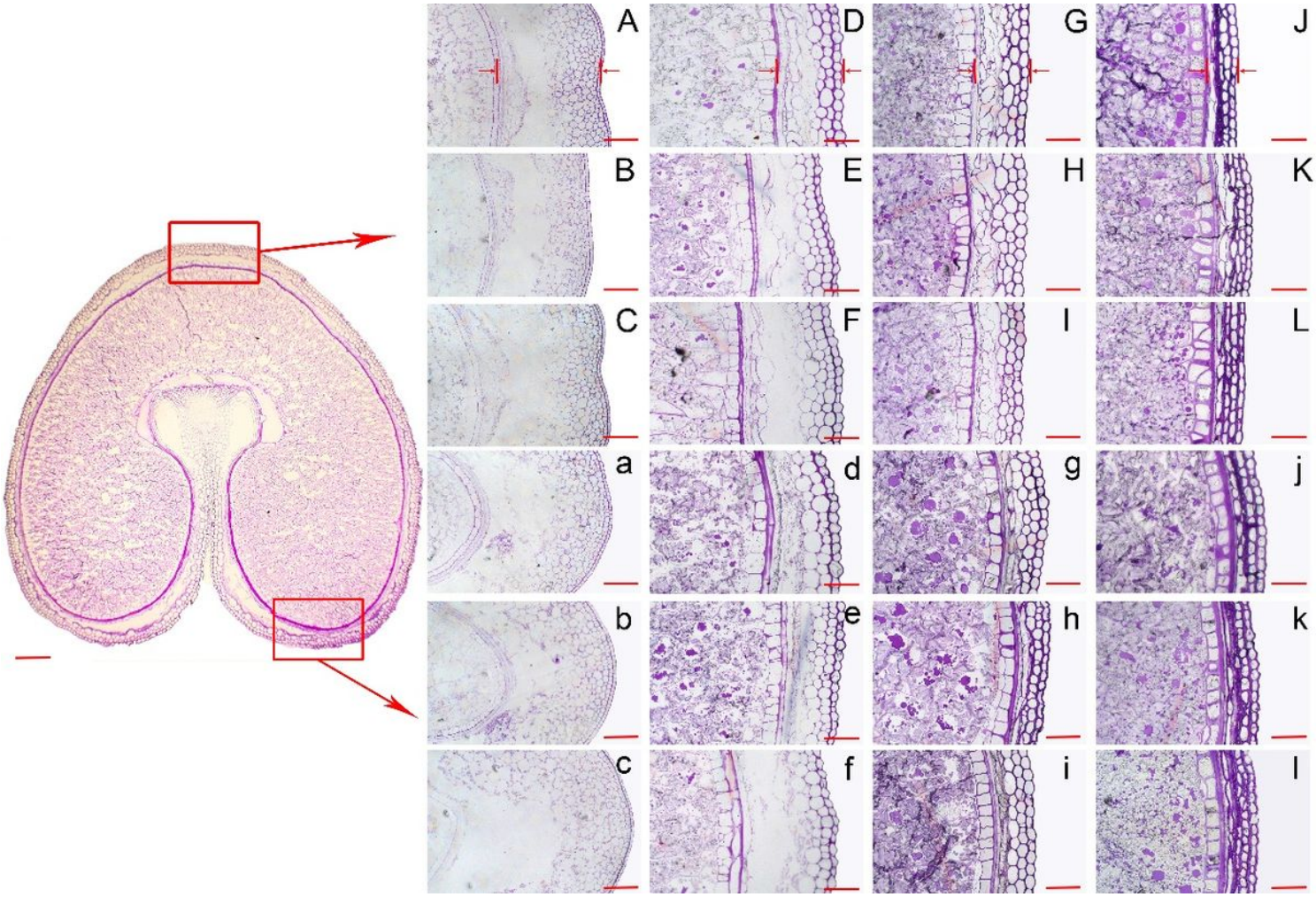

Figure 1

Observation of the microstructure of the dorsal and abdomen pericarps of caryopsis at different stages. Figure A-L was the dorsal pericarp structure and Figure a-l was the abdominal pericarp structure. The rows were the slice structures of G1, G2, and G3, and the columns were the slice structures of 8, 14, 20, and 30 DAA. Bar: 10 μm.

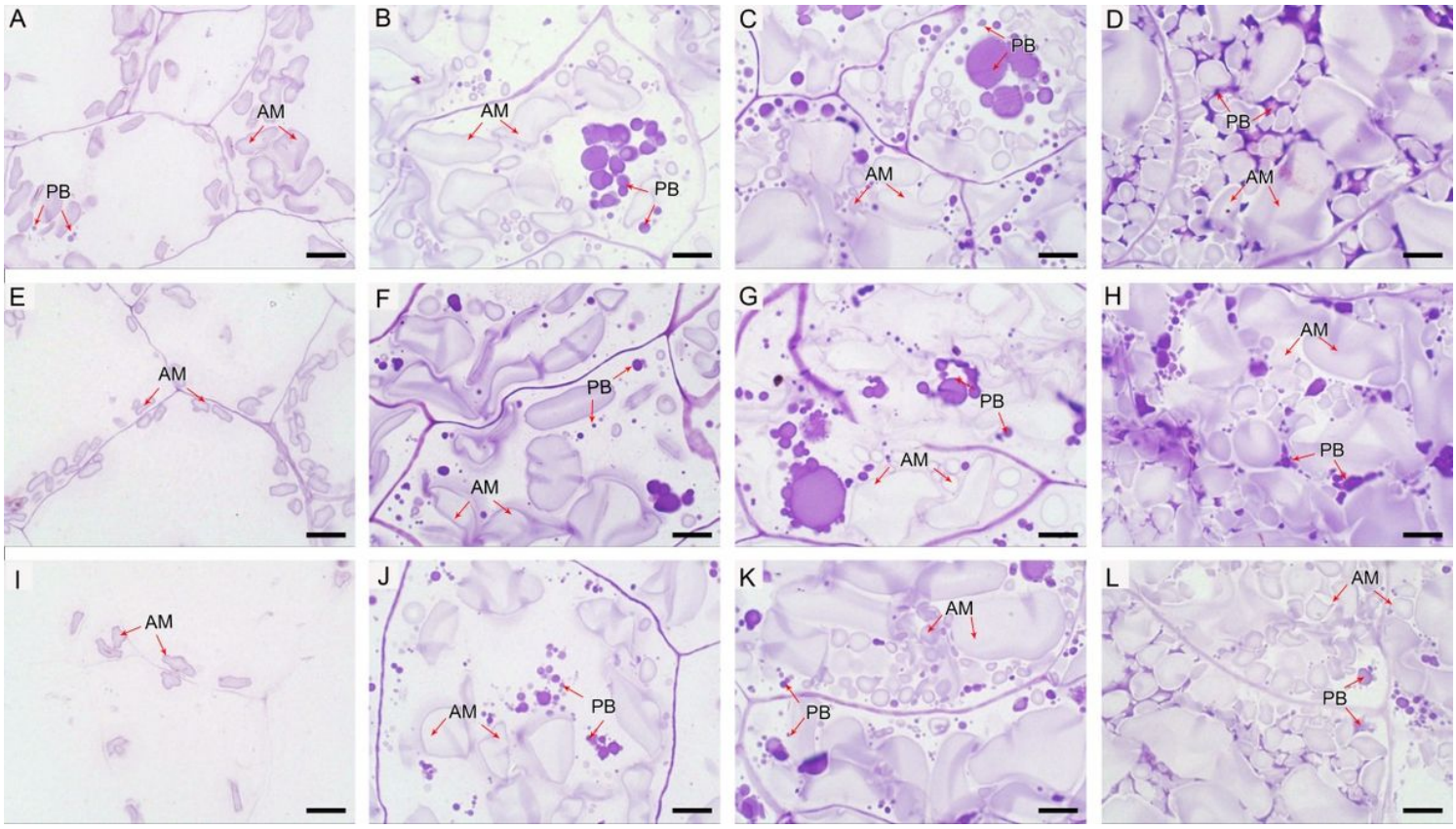

Figure 2

Endosperm development at different developmental stages of different grain positions A-D, E-H, I-L was the abdominal endosperm of the G1, G2, and G3 of 8, 14, 20, and 30 DAA, respectively. Am: amyloplast, PB: protein body. Bar: 0.1 μm.

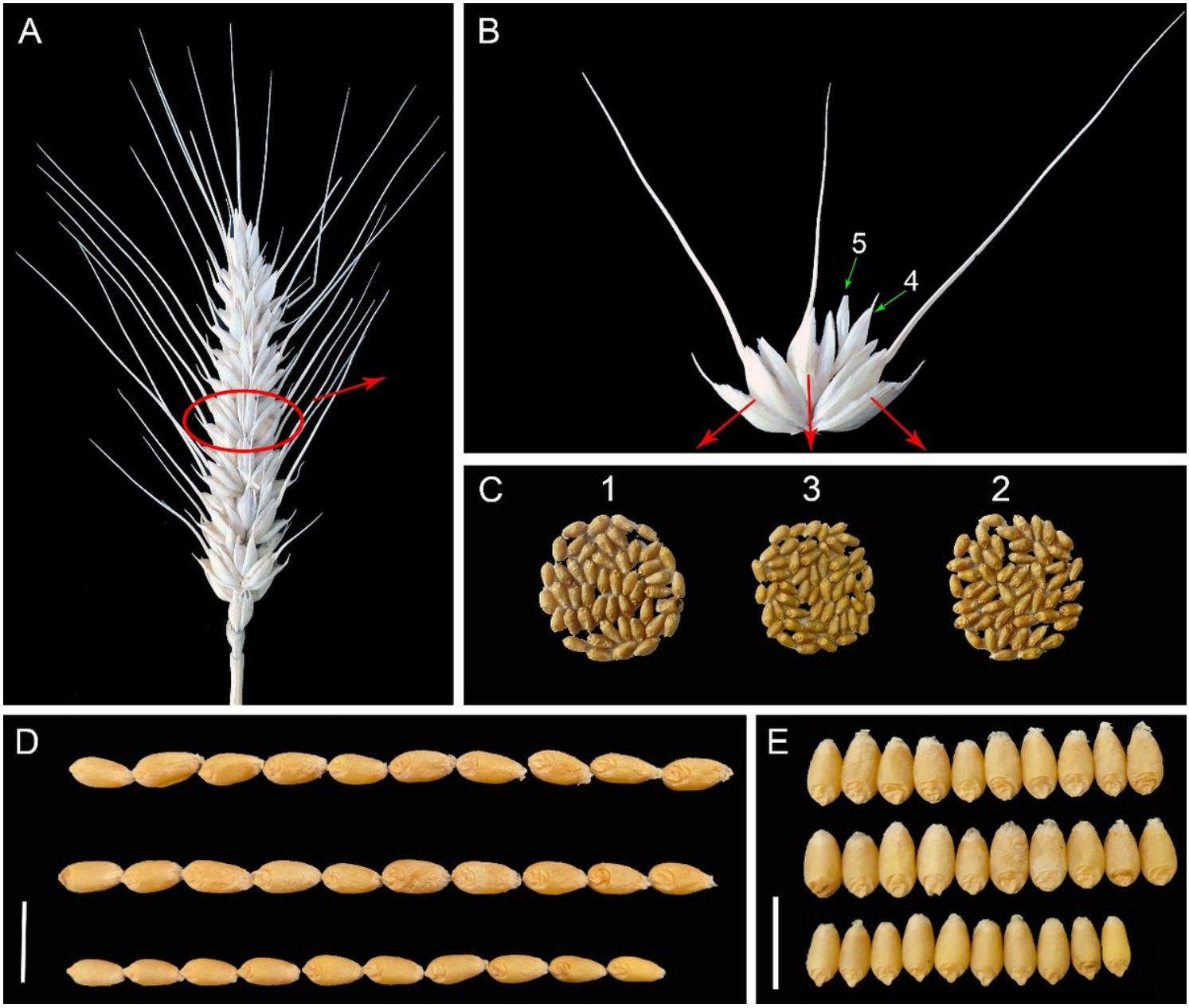

Figure 3

Division of wheat grain positions and observation of grain morphology. Figure A presents a mature wheat spike. Figure B shows the division of the grain position in wheat spikelet. Figure C shows the grain corresponding to the grain position. Figures D and E present the comparisons of the lengths and widths of 10 grains in different positions. Bar: 10 mm.

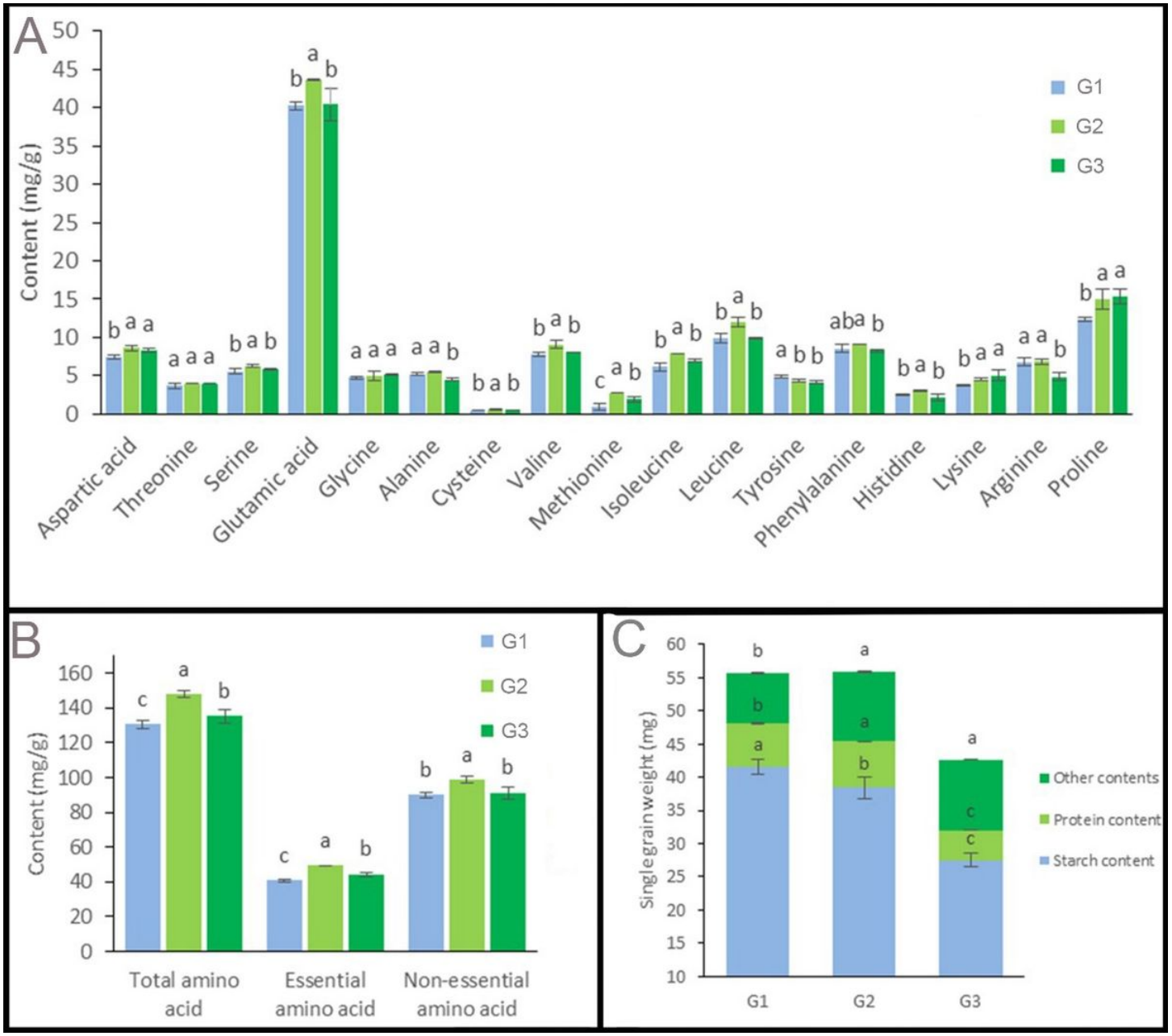

Figure 4

Determination of amino acid content in mature grains of different grain positions and accumulation of single grains. Figure A shows the content of each amino acid in different grain positions; Figure B shows the total, essential, and non-essential amino acid contents; and Figure C shows the accumulation of substances in a single grain.

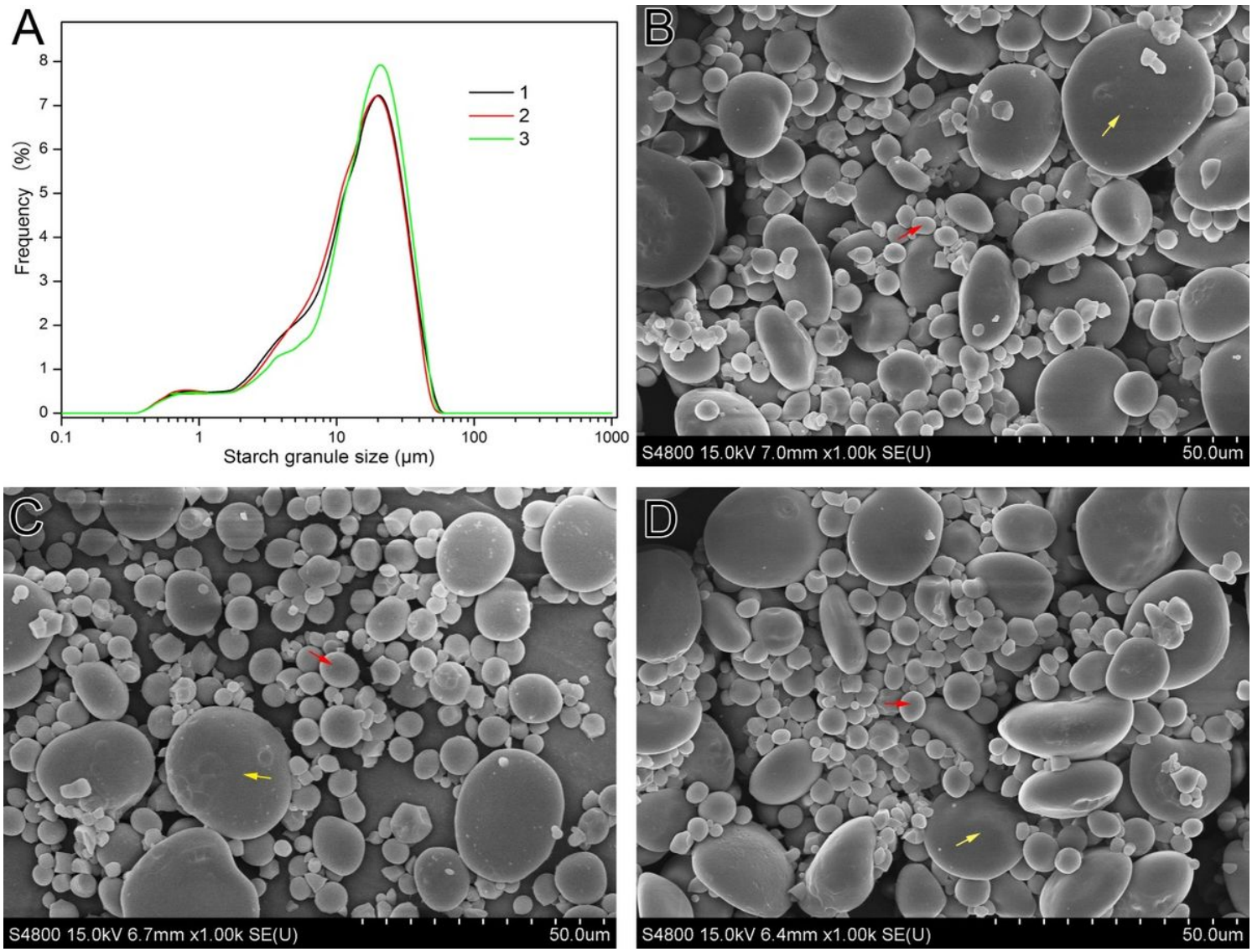

Figure 5

Granule size distribution diagram and morphological structure observation of each grain starch. Figure A shows the granule size distribution of starches, Figures B, C, and D show the morphology of G1, G2, and G3, respectively.

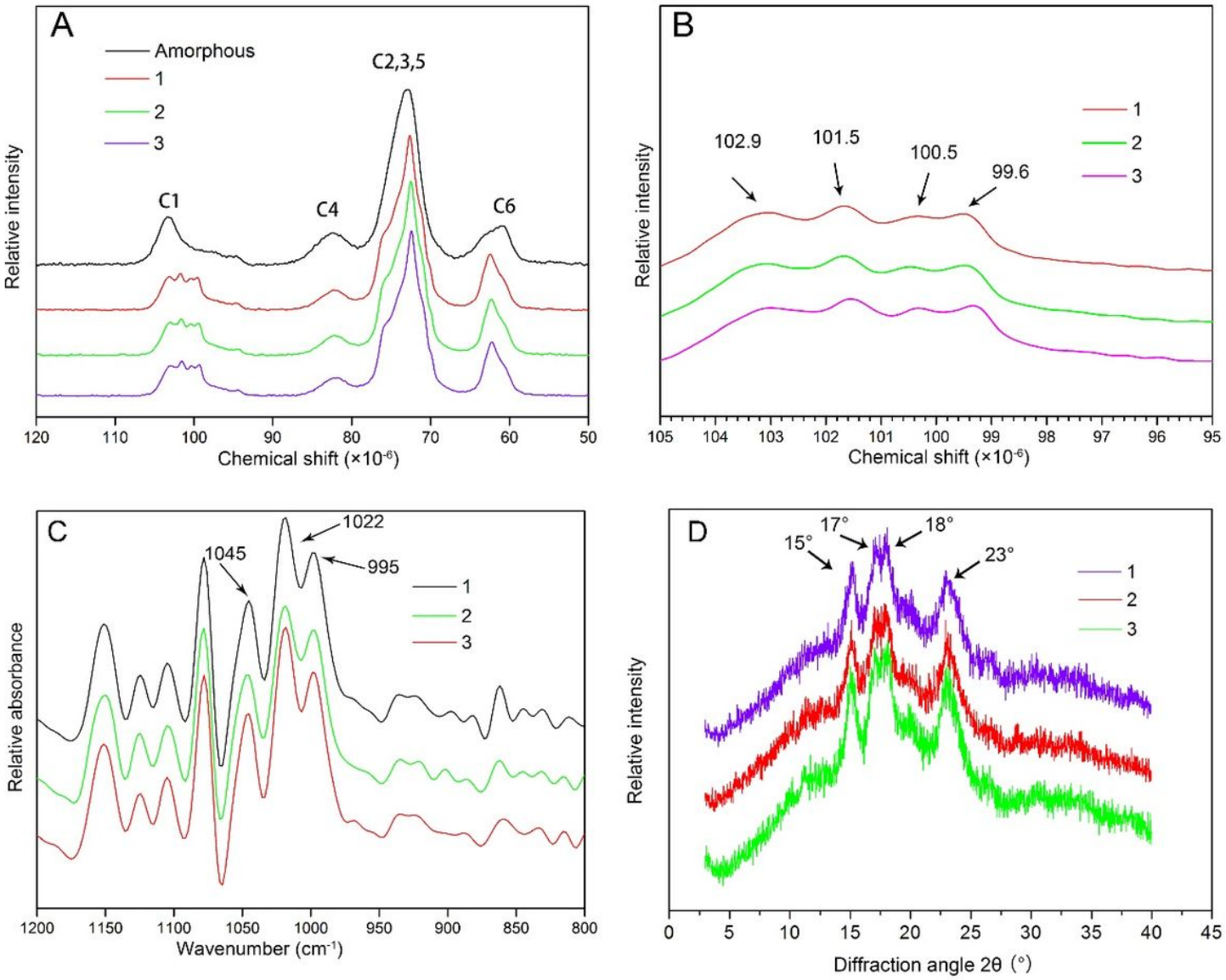

Figure 6

Starch CP/MAS 13C NMR spectroscopy (A-B), FTIR (C) and XRD patterns (D) in different grain positions. Lowercase numbers 1, 2, and 3 represent G1, G2, and G3, respectively.

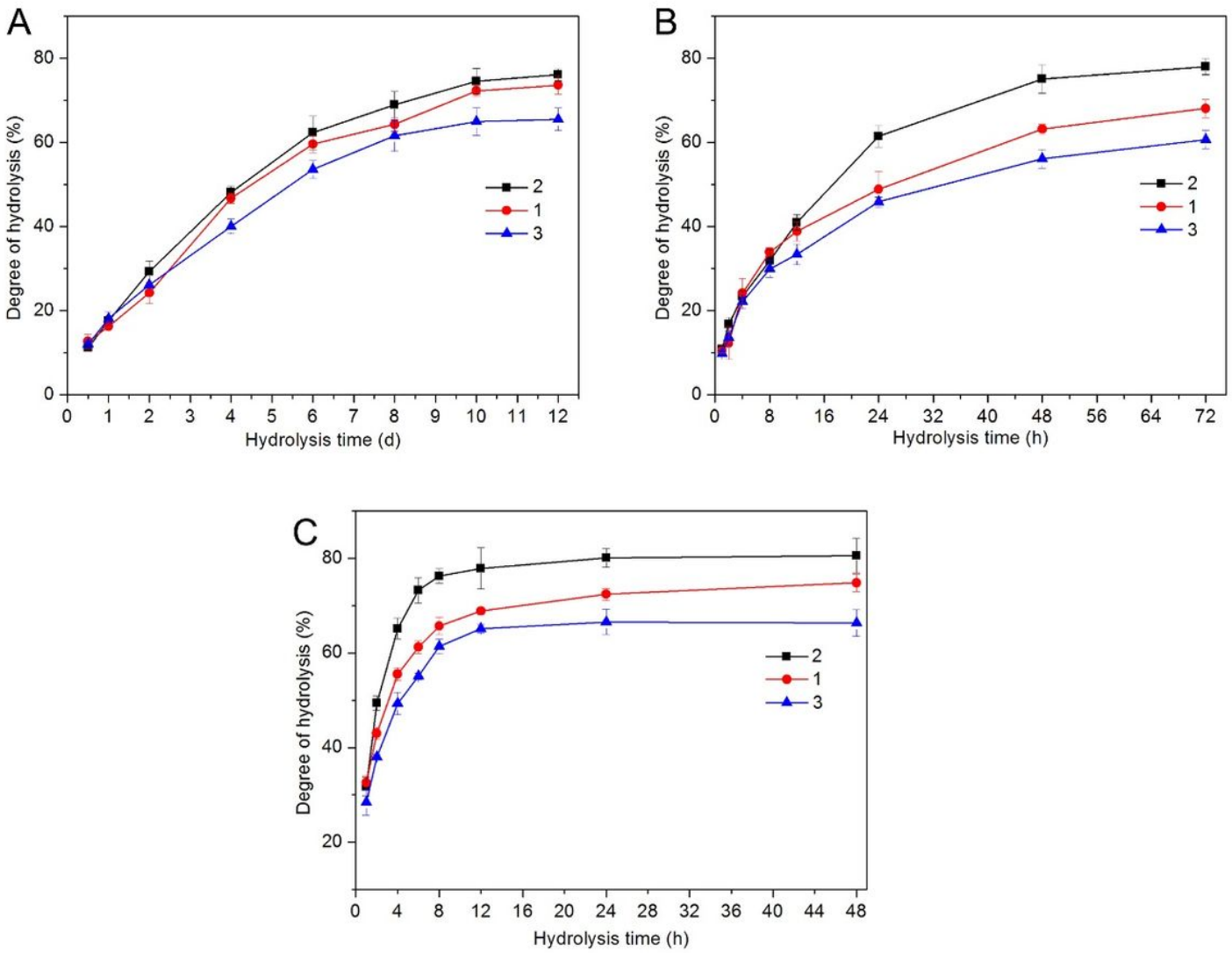

Figure 7

A, B, C were degree of hydrolysis by HCL, PPA, AAG. Lowercase numbers 1, 2, and 3 represent G1, G2, and G3, respectively.